Minimal Mechanisms Responsible for the Dispersive Behaviour of the Madden Julian Oscillation

Vincent Mathew * and Kartheek Mamidi

Posted Date: 8 August 2023

doi: 10.20944/preprints202308.0626.v1

Keywords: Madden Julian Oscillation; shallow water model; moisture interactions

Article

Minimal Mechanisms Responsible for the Dispersive Behaviour of the Madden Julian Oscillation

Kartheek Mamidi and Vincent Mathew*

Department of Physics, Central University of Kerala, Periye, Kasaragod 671316 Kerala, India

* Correspondence: vincent@cukerala.ac.in

Abstract: An attempt has been made to explore the relative contributions of moisture feedback processes on tropical intraseasonal oscillation or Madden Julian Oscillation (MJO). We focused on moisture feedback processes, including evaporation wind feedback (EWF) and moisture convergence feedback (MCF), which integrates the mechanisms of convective interactions in the tropical atmosphere. The dynamical framework considered here is a moisture-coupled, single-layer linear shallow-water model on an equatorial beta-plane with zonal momentum damping. With this simple approach, we aimed to recognize the minimal physical mechanisms responsible for the existence of the essential dispersive characteristics of the MJO, including its eastward propagation($k > 0$), the planetary-scale (small zonal wavenumbers) instability, and the slow phase speed of about ≈ 5 m/sec. Further, we extended our study to determine each feedback mechanism's influence on the simulated eastward dispersive mode. Our model emphasized that the MJO-like eastward mode is a possible outcome of the combined effect of moisture feedback processes without requiring additional complex mechanisms such as cloud radiative feedback and boundary layer dynamics. The results substantiate the importance of EWF as an energy source for developing eastward moisture mode with a planter-scale instability. Moreover, our model endorses that the MCF alone could not produce instability without surface fluxes, although it has a significant role in developing deep convection. It is found that the MCF exhibits a damping mechanism by regulating the frequency and growth rate of the eastward moisture mode at shorter wavelengths.

Keywords: Madden Julian Oscillation; shallow water model; moisture interactions

1. Introduction

Low-frequency moisture modes or intraseasonal oscillations (ISO) in the tropical atmosphere refer to persistent and coherent patterns of atmospheric variability that occur on a typical time scale of around 60-120 days [1]. These modes are characterized by fluctuations in atmospheric circulation and precipitation patterns that can substantially impact regional and global climate. The Madden-Julian Oscillation (MJO), for example, is a large-scale ISO characterized by a pattern of enhanced and suppressed convection and rainfall that moves across the tropical Indian Ocean and Western Pacific on a time scale of about 30 to 60 days [2,3]. The MJO affects the distribution and transport of moisture in the atmosphere and can significantly impact monsoon systems and other precipitation patterns.

Modern satellite technology could provide spectral analysis results, which reveal the strong connection between large-scale tropical motions and moist convection [4]. The linear dispersion relation of these tropical modes was successfully derived more than half a century ago by Matsuno [5], using a "classical dry" linear equatorial beta-plane shallow-water model. However, Matsuno's "dry" theory cannot deduce the observed moist tropical modes with lower phase speeds. With the help of normalized power spectra of satellite data, such as Outgoing Long-wave Radiation (OLR), Kiladis *et al.* [4] showed that the family of linear wave solutions predicted by Matsuno was characterized by deep convection in the tropics. Hence, these observed modes are later referred to as Convectively Coupled Equatorial Waves (CCEWs).

For the past several decades, there has been significant research on the dynamics, structure, and propagation characteristics of CCEWs in observation and theoretical studies. Aside from CCEWs,

 doi:10.20944/preprints202308.0626.v1

Hendon and Salby [6] and Kiladis *et al.* [7] observed a dominant mode of tropical variability in the wavenumber-frequency spectra of OLR, concentrated on the intraseasonal time scale and the planetary zonal scale and this dominant signal is referred to as MJO. However, unlike other tropical modes, the MJO does not fall along Matsuno's classical dispersion curve and has a peculiar dispersion, i.e., frequency is nearly constant with increasing positive zonal wavenumber in a low-frequency regime. The MJO is an organized, eastward propagating ($\simeq$ 5 m/sec), large-scale convective envelope, and it is embedded with both east and westward-moving convective fine-structures, making it a complex phenomenon to understand [8,9]. Due to its multi-scale moisture-driven structure, it impacts the local and global climatic variabilities and provides a significant source of predictability at intraseasonal scales [10]. During the last few decades, through observational research, scientists have evaluated the impact of MJO on phenomena ranging from diurnal convective events to large-scale motions such as monsoon variability, tropical cyclones, and extra-tropical circulations [11–13].

Since its first observation, MJO inspired many researchers to develop a theory for representing its fundamental dynamics [14]. Some scientists have attempted to explain the MJO as an additional eastward propagating moisture mode of the tropical wave spectrum and addressed its underlying physical mechanisms. These theories have relied on either Matsuno's original representation of classical dry trapped waves or the same linear approach with an additional set of equations by including moisture as a new variable. This school of theories includes moisture-mode theories [15–19], trio-interaction theories [20], skeleton theory [13], and WISHE-moisture mode theories [21–24]. However, another school of theories also exists in which the authors explained the MJO dynamics through various physical mechanisms without using moisture as an additional variable, such as gravity wave theory by Yang and Ingersoll [25] and non-linear solitary wave theory of Yano and Tribbia [26], Rostami and Zeitlin [27].

The two-way interaction between the convection and moisture dynamics is the non-trivial and most debated problem in the field of tropical atmospheric research since the development of conditional instability of second kind (CISK)-mechanism by Charney and Eliassen [28] and Ooyama [29]. In one-way, moisture dynamics in the tropical atmosphere play a key role in shaping convective interactions. Conversely, convective dynamics can help sustain and amplify low-frequency ISOs by influencing the distribution and transport of moisture, heat, and energy in the atmosphere. In CISK theory, they established that convection due to latent heat release leads to the development of large-scale motion when there is ambient conditional instability. However, Emanuel *et al.* [30] contradicted the representation of convection in the earlier CISK mechanism, stating that convection acts as a damping source to sustain the large-scale instability and coined the term moist convective damping in his wind-induced surface heat exchange (WISHE) theory.

In tune with the aforementioned linear CISK theory, Lindzen [31] developed a Wave-CISK by emphasizing the role of latent heat release, but the obtained linear solution suffered by the ultraviolet catastrophe of largest growth at the smallest scales. Later on, Moskowitz and Bretherton [32] rectified this unrealistic solution by including frictional convergence to the wave-CISK mechanism. However, in their earlier works, this theory was continuously criticized by Emanuel [21] for the requirement of background conditional instability and treatment of the convective dynamics [33,34]. Meanwhile, [21] developed a new paradigm, in which large-scale motions in the tropics were driven by an energy source known as WISHE or evaporation-wind feedback (EWF). Further, Sobel and Maloney [17], Khairoutdinov and Emanuel [24], Fuchs-Stone and Emanuel [35] successfully explored the role of evaporation fluxes as a primary mechanism in MJO dynamics. In the earlier linear analysis of Fuchs and Raymond [22], they initially thought MJO is an outcome of the combined effect of cloud radiation feedback (CRF) and WISHE. Later, they established that CRF shows a destabilizing mechanism at the same time, WISHE develops a primary instability [23]. However, the interaction between radiation and water vapor goes back to the earlier hypothesis of Hu and Randall [36]. Further, Adams and Kim 2016 extended this mechanism by modifying the CRF as a function of wavenumber in their moisture mode theory and established the importance of CRF on MJO dynamics. The role of CRF has been

Preprints (www.preprints.org) | NOT PEER-REVIEWED | Posted: 8 August 2023 doi:10.20944/preprints202308.0626.v1

explored in other theoretical frameworks as well, such as trio-interaction models by [20] with the inclusion of planetary boundary layer (PBL) dynamics. In this formulation, the authors concluded that the combination of the CRF and PBL leads to the development of planetary scale instability, and the phase speed and growth rates are influenced by CRF mechanism[37].

Despite the fact that there is a large and diversified pool of theoretical works to draw from, numerous questions remain unsolved (for a complete overview, readers can refer to Zhang *et al.* [14]). As a result, understanding the MJO's dynamics remains a challenge and is considered the "Holy Grail" of tropical atmospheric research [15]. However, the primary goal of this work is not to answer all of the unanswered questions about MJO dynamics. Instead, we intend to evaluate the bare-bone physical mechanisms responsible for recreating the MJO's dispersive signature. According to Nakazawa [38] and Lindzen [31], low-level moisture convergence is an essential physical process within the tropics, which plays a crucial role in shaping convective dynamics and further influences the large-scale dynamics of low-frequency tropical modes. Here, we aim to explore the possibility of visualizing the MJO as an intrinsic mode introduced by moisture feedback processes while encompassing the significance of evaporation-wind feedback and low-level moisture convergence in the tropical atmosphere. The individual roles of the above mechanisms have been demonstrated extensively in earlier theories. However, the possible role of each mechanism and combination of one another in determining the dispersive signature of MJO-like mode is still elusive. Here we established the simple mathematical description, which estimates each mechanism's possible role and strength, and also in combination with one another in exhibiting the MJO-like mode.

The paper is organized as follows. Assuming a simple first baroclinic structure, in the next Section 2, we have introduced the system of equations, which describes the dynamics of the tropical waveguide, and we proceed to linear analysis. We have explored the dispersion relation and associated moisture mode characteristics. Results are discussed in Section. 3. Finally, the concluding remarks are given in Section. 4.

2. Theoretical Description

The theoretical framework presented here represents the low-frequency intraseasonal oscillations in the tropical atmosphere. It describes the horizontal structure of the first baroclinic mode in the tropics. It consists of simplified parameterizations of evaporation-wind feedback and precipitation heating in a nearly saturated convective tropical atmosphere [39]. These approximations are applied to rotating shallow water equations on an equatorial β - plane, along with an equation for the depth-integrated moisture variable. The complete, dimensional form of the described model is as follows:

$$\frac{D\mathbf{V}}{Dt} + f \times \mathbf{V} = \nabla\phi - \epsilon\mathbf{V} \tag{1}$$

$$\frac{\partial\phi}{\partial t} - \nabla.(\phi\mathbf{V}) = Q - \mu\phi \tag{2}$$

$$\frac{\partial q}{\partial t} + \nabla.(\mathbf{V}\mathbf{q}) = \mathbf{E} - \mathbf{P} \tag{3}$$

Equation (1) represents the zonal and meridional momentum equations with linear mechanical damping, where $\mathbf{V}(\mathbf{u}, \mathbf{v})$ represent the free-tropospheric low-level zonal and meridional velocity perturbations. Equation (2) is derived from continuity, hydrostatic and thermodynamic equations with ϕ as a mid-level mean potential temperature, where μ is the Rayleigh friction and Q as the heating rate due to condensation. Equation (3) is the vertically integrated moisture equation, which describes the evolution of the moisture variable q, and here E represents the evaporation, and P represents the

Preprints (www.preprints.org) | NOT PEER-REVIEWED | Posted: 8 August 2023 doi:10.20944/preprints202308.0626.v1

precipitational heating. We adopted the simplified treatment of parameterization schemes for these source terms similar to previous moist models [40], and are given by

$$Q = \eta P \tag{4}$$

where,

$$\eta = \frac{L_v}{\rho_a C_p H}$$

Here L_v is the latent heat of condensation, ρ_a is the density of air, and C_p is the specific heat at constant pressure. The precipitational anomaly is completely governed by the moisture relaxation time (τ), and according to the Bretherton *et al.* [41], the expression is given by

$$P = \frac{\bar{q}s}{\tau} \tag{5}$$

where, s describes the evolution of the perturbation moisture variable, and is obtained from the relation $q = \bar{q}$ (1+s), where $\bar{q}$ is the equilibrium value of moisture variable q.

The surface evaporation is parameterised by the simplified bulk-aerodynamic formula [42,43], and given by

$$E = -\rho_a C_D \Delta\bar{q}_s.|\vec{u}| \tag{6}$$

Where C_D is the drag coefficient and $\Delta\bar{q}_s$ (= 3 $g\ kg^{-1}$) is the saturation relative humidity difference between the sea surface and the anemometer level. The evaporation term's sign depends on the direction of the background mean wind $|\bar{u}|$, and it is positive (negative) sign for mean easterlies (westerlies). For analytical simplicity, we assume that strong easterly wind anomalies ($\Lambda > 0$) are the dominant mean background winds in the lower troposphere tropical circulation [44].

Since the major objective of our study is to investigate the linear modes in a low-frequency regime, we linearized the equations (1) - (3) and used the long-wave approximation. We further neglected the zonal moisture advection term, in order to focus on the role of EWF and MCF in linear wave dispersion. Therefore, The reduced governing equations for studying the moist tropical modes are as follows

$$\left(\frac{\partial}{\partial t} + \epsilon^*\right) u - f^* v - \frac{\partial \phi}{\partial x} = 0 \tag{7}$$

$$f^* u - \frac{\partial \phi}{\partial y} = 0 \tag{8}$$

$$\left(\frac{\partial}{\partial t} + \mu^*\right) \phi - \{\frac{\partial u}{\partial x} + \frac{\partial v}{\partial y}\} - \eta\alpha s = 0 \tag{9}$$

$$\frac{\partial s}{\partial t} + \Gamma_q \{\frac{\partial u}{\partial x} + \frac{\partial v}{\partial y}\} + \Lambda u + \alpha s = 0 \tag{10}$$

where,

$$\Gamma_q = 1 - \left[\frac{H}{\bar{q}}\right] \frac{d\bar{q}}{dz}$$

The parameter Λ represents the non-dimensional values of the evaporation-wind feedback component, estimated from the empirical relation given in Table 1. α is the non-dimensional value of the moisture relaxation timescale, ϵ^* represents the linear mechanical damping parameter, μ^* is the Rayleigh friction

Preprints (www.preprints.org) | NOT PEER-REVIEWED | Posted: 8 August 2023 doi:10.20944/preprints202308.0626.v1

or Newtonian cooling and Γ_q is the moisture convergence feedback. The list of model parameters, including non-dimensional parameters, and their values are given in Table 1.

Table 1. Description of the model parameters.

Description	Parameter	Definition/Units	Average Value
Dry gravity wave speed	C	ms^{-1}	50
Time scale	T_0	$[2C\beta]^{\frac{1}{2}}$	8.33 hours
Length scale	L_0	$[\frac{C}{2\beta}]^{\frac{1}{2}}$	40,000 km
Meridional gradient of Coriolis parameter	β	$m^{-1}s^{-1}$	2.28×10^{-11}
Moisture convergence feedback*	Γ_q	$1-(\frac{H}{\bar{q}})\frac{d\bar{q}}{dz}$	-0.05
Convective time lag*	α	$[\frac{T_0}{\tau}]$	0.25
Rayleigh Damping*	ϵ^*	$[\frac{T_0}{T_d}]$	0.04
Evaporation-wind feedback*	Λ	$\rho C_D \Delta\bar{q}_s \frac{T_0}{\bar{q}}$	0.05

* for Nondimensional Parameters

2.1. Dispersion Relation

Equations (7) - (10) represent a closed system of linear partial differential equations with constant coefficients. We assume that solutions have a zonally propagating plane-wave structure of the form $\zeta(x,y,t) = \zeta(y)e^{[i(kx-\omega t)]}$, where ζ represents any of the perturbed variables u, v, θ, or s. "k" is the zonal wavenumber $k = 1, 2, 3, \ldots$ and ω is the complex frequency. The phase speed and growth rate can be deduced by real part $Re(\omega)/k$ and imaginary parts $Im(\omega)$ of the frequency ω. For simplicity, we considered the time scale for mechanical damping and Newtonian cooling to be the same ($\epsilon = \mu = \epsilon^*$). Therefore, we can write the linear system of equations in terms of frequency and wavenumber as.

$$\sigma u - if^* v + k\phi = 0 \tag{11}$$

$$f^* u - \frac{d\phi}{dy} = 0 \tag{12}$$

$$\sigma\phi + ku - i\frac{dv}{dy} - i\eta\alpha s = 0 \tag{13}$$

$$\omega^* s - [k\Gamma_q - i\Lambda]u + i\Gamma_q \frac{dv}{dy} = 0 \tag{14}$$

with

$$\sigma = \omega + i\epsilon^*; \quad \omega^* = \omega + i\alpha$$

By eliminating the variable s from Equations (13) - (14), we can achieve new system of equations, further conducting the mathematical manipulation and eliminating the variable ϕ results a second order ordinary differential equation in $v(y)$.

$$\frac{d^2v}{dy^2} + a_0 y\frac{dv}{dy} + a_1 v = 0 \tag{15}$$

while the parameters

$$a_0 = \frac{\bar{\Lambda}}{\sigma\bar{\Gamma}}; \qquad a_1 = -\left[\frac{\bar{\Gamma}}{\sigma\Gamma} + \frac{1}{\Gamma}\right]$$

Preprints (www.preprints.org) | NOT PEER-REVIEWED | Posted: 8 August 2023 doi:10.20944/preprints202308.0626.v1

Further, by applying the variable transformation we can achieve a reduced second order differential equation in $V(\psi)$. Which is similar to the Matsuno's equation,

$$\frac{d^2V}{d\psi^2} + (C_2 - C_1\psi^2)V = 0 \tag{16}$$

The coefficients C_1 and C_2 are

$$C_1 = \frac{1}{\bar{\Gamma}} - \left[\frac{\bar{\Lambda}}{2\sigma\bar{\Gamma}}\right]^2; \quad C_2 = -\left[\frac{\bar{\Gamma}}{\sigma\bar{\Gamma}} + \frac{\bar{\Lambda}}{2\sigma\bar{\Gamma}}\right]$$

where,

$$\bar{\Gamma} = \Gamma k - \bar{\Lambda};$$
$$\bar{\Lambda} = \frac{\eta\alpha\Lambda}{\omega^*}; \quad \Gamma = 1 - \frac{i\eta\alpha\Gamma_q}{\omega^*}$$

However, we assume a wave motions near to the equatorial region and we apply the boundary conditions such as $V \to 0$, when $\psi \to \pm\infty$. With these boundary conditions, the solution to the above Hermite differential equation can be either of the form,

$$V = 0; \text{or} \quad V(\psi) = Ce^{-c_n y^2} H_n(\psi) \tag{17}$$

where $H_n(\psi)$ is the nth-order Hermite polynomial. The solution given by Equation (17) is possible only when it satisfies the following relation

$$C_2 C_1^{-1/2} = 2n + 1; \quad n = -1, 0, 1, 2, \ldots \tag{18}$$

where n is an integer, which represents the meridional mode.

Solving Equation (18) results the dispersion relationship, and it can be written as a characteristic polynomial in ω as follows

$$N^2\omega^4 - a_0\omega^3 - a_1\omega^2 - a_2\omega + a_3 = 0 \tag{19}$$

where the coefficients a_0, a_1 a_2 a_3 are as follows,

$$a_0 = iN^2[\alpha(1+\Delta) - 2\epsilon^*],$$

$$a_1 = [k^2 + N^2(\epsilon^{*2} + \alpha^2 + 4\epsilon^*\alpha - 2\epsilon^*\eta\alpha\Gamma_q - \eta\alpha^2\Gamma_q)],$$
$$a_2 = 2i\alpha k^2\Delta - \eta\alpha\Lambda k + iN^2[\epsilon^{*2}\alpha(1+\Delta) + 2\epsilon^*\alpha^2\Delta],$$

$$a_3 = \alpha^2k^2[1 - 2\eta\Gamma_q + \eta^2\Gamma_q] + i\eta\alpha^2\Lambda k\Delta - \frac{(1+N^2)}{4}\eta^2\alpha^2\Lambda^2 + N^2\epsilon^{*2}\alpha^2\Delta$$

with

$$N = 2n + 1; \quad \Delta = 1 - \eta\Gamma_q$$

3. Results and Discussion

Before examining the complete dispersion relation in detail, we consider the limiting case with no feedback processes, i.e., neglecting the precipitational heating, moisture convergence (Γ_q = 1), evaporation-wind feedback (Λ = 0), and mechanical damping (ϵ = 0). This approximation results in reduced classic Matsuno's dispersion equation ($\omega^2 - k^2 = 0$) for a special case of zero meriodonal wind ($v = 0$). This dispersion relation, illustrates that in the absence of feedback processes, the solution exhibits a nondispersive eastward propagation, and this mode's behavior closely resembles

Preprints (www.preprints.org) | NOT PEER-REVIEWED | Posted: 8 August 2023 doi:10.20944/preprints202308.0626.v1

the pattern followed by the dry Kelvin mode of Matsuno [5]. Hence, we argue that the additional physical mechanisms, such as moisture feedback processes (EWF and MCF), which could provide an energy source, are required to develop an eastward instability at the planetary scale.

We further studied the specific solutions of Equation (19) using the standard parameter set detailed in Table 1. The solutions are shown in Figure 1a, where the real part of frequency (Re(ω)) is plotted against zonal wavenumber (k), and the corresponding growth rate is shown in Figure 1b. We obtained two modes of solution in the low-frequency domain; one is propagating in the westward direction ($k < 0$), and the other in the eastward direction ($k > 0$). The observed wave mode closest to the modeled westward branch (blue dots) in the low-frequency regime is the n = 1 traditional moist Equatorial Rossby wave. The additional low-frequency eastward moisture mode is unstable at planetary-scale zonal wavenumbers ($k \leq 2$) with a frequency that is weakly dependent on the zonal wavenumber. Both the low-frequency modes show the highest growth rate at longer wavelengths ($k <$ 2) and slowly fall at shorter wavelengths ($k > 4$). However, the eastward mode (blue open circles) shows the maximum growth rate compared to the westward mode. Hence, from this illustration, it is clear that the manifestation of the eastward low-frequency mode is due to the existence of moisture feedback processes.

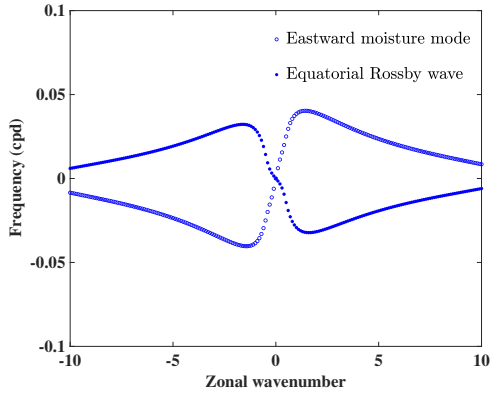

(a) Frequency (cycles per day) of eastward mode (blue open circles) and westward mode (blue dots)

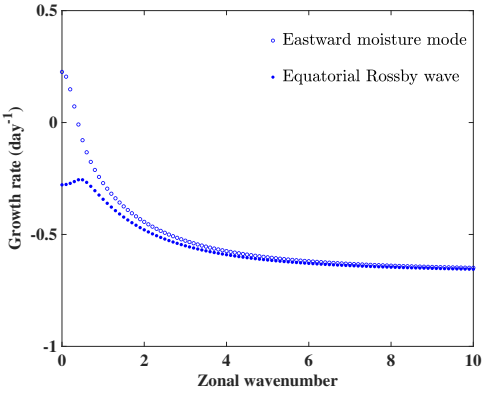

(b) Growth rate (day^{-1}) of eastward mode (blue open circles) and westward mode (blue dots)

Figure 1. The Low-frequency modes of $\omega(k)$ versus k from Equation 19: when α = 0.25, Γ_q = -0.05, Λ = 0.05, and ϵ = 0.04.

The dynamic features of the eastward mode are shown in Figure 2. The new eastward propagating mode has a period within the intraseasonal range (Figure 2a). It is an unstable mode with the maximum growth rate at longer wavelengths, indicating a preferred planetary-scale unstable mode (Figure 2b), and the dimensional phase speed at planetary-scale wavenumber is nearly 5 m/sec (Figure 2c). This distinct dispersive signature is consistent with the fundamental characteristics of the MJO predicted and simulated by various theoretical studies such as Raymond and Fuchs [15], Sobel and Maloney [17] and also Wang *et al.* [20]. Based on the minimum criteria and desirability formulated by Zhang *et al.* [14], we identify our eastward moisture mode as MJO-like. Our model's eastward moisture mode solution is similar in nature to the linear solutions of WISHE-moisture mode theory and BLQE theory with a zero meridional wind ($v = 0$) approximation of Fuchs and Raymond [23], Fuchs-Stone [45], and also similar to the $n = 1$ mode of Fuchs-Stone and Emanuel [35], Emanuel [44] with a meridional flow. Most importantly, both models are in the common paradigm that cloud-radiation interaction (CRI) and WISHE mechanisms are responsible for developing and maintaining planetary scale instability. However, our theoretical formulation did not involve complex cloud-radiation and boundary layer dynamics. Nevertheless, we obtained a similar solution.

Preprints (www.preprints.org) | NOT PEER-REVIEWED | Posted: 8 August 2023 doi:10.20944/preprints202308.0626.v1

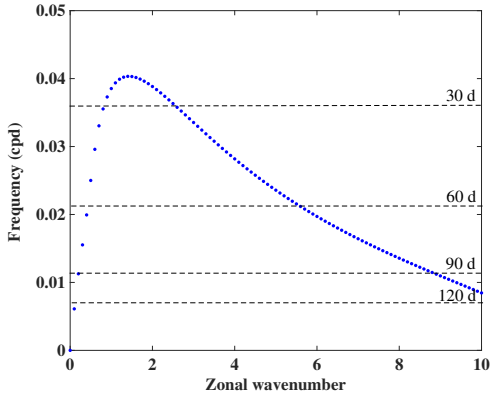

(a) Frequency (cycles per day)

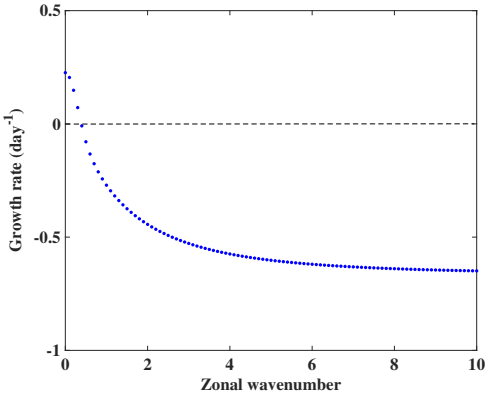

(b) Growth rate (day^{-1})

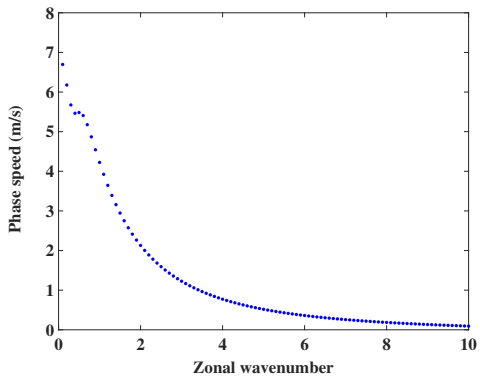

(c) Phase speed (m/sec)

Figure 2. The eastward propagating moisture mode: when α = 0.25, Γ_q = -0.05, Λ=0.05, and ϵ = 0.04.

From Figure 2, It is clear that the existence of eastward moisture mode and its planetary-scale instability is due to the competing mechanism between the moisture feedback processes. Therefore, we intend to identify the individual roles of the MCF and EWF. We first exclude the EWF (by setting Λ to zero) and by invoking the MCF alone. This approximation results in an unrealistic solution Figure 3a (blue open circles), which explains that there is no energy source for an eastward moisture mode to grow when the EWF is absent (Λ = 0) even though MCF is active. This result agrees with earlier theoretical works based on the WISHE theory. Further, we varied EWF values by holding the other parameters as constant, which resulted in a modified eastward mode with respect to EWF, illustrated in Figure 3b. It shows that for higher values of EWF, such as Λ = 1.5 and 3, the obtained mode has a typical instability and exhibits nonlinearity at planetary-scale wavelengths. Similarly, the growth rate curves show maximum growth at planetary-scale wavelengths ($k > 3$) for increasing the Λ values. However, the modified mode gets damped for intermediate and shorter wavelengths (Figure 3c). Increasing the EWF values up to 1 ($\Lambda < 1$) does not influence the fundamental behavior of the eastward moisture mode. i.e., the phase speed decreases with increasing wavenumber for $\Lambda < 1$, with a maximum phase speed at longer wavelengths, retained the same. However, the Λ values above 1.5 exhibit very slow-phase speed in longer wavelength ranges $k < 1.5$, further attaining maximum phase speed at $k > 1.5$ and then decreasing slowly with the wavenumber. This typical behavior explains the nonlinear nature of the mode at longer wavelengths. We then tested the negative value of EWF (by setting $\Lambda < 0$), which results in similar nature of Λ = 0, with an unrealistic dispersion relation (blue dots). Therefore, the EWF mechanism is solely responsible for the development of planetary-scale instability in our model.

Preprints (www.preprints.org) | NOT PEER-REVIEWED | Posted: 8 August 2023 doi:10.20944/preprints202308.0626.v1

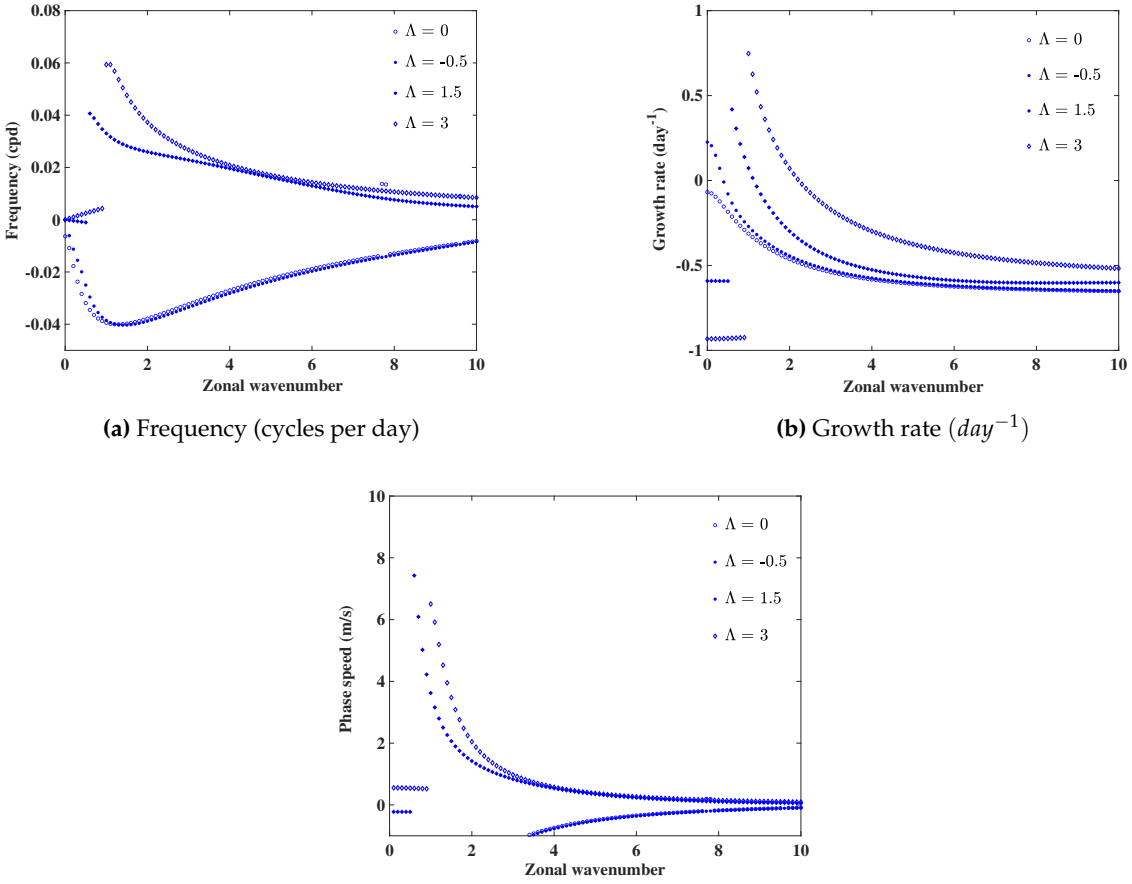

(a) Frequency (cycles per day)

(b) Growth rate (day^{-1})

(c) Phase speed (m/sec)

Figure 3. The role of feedback parameter EWF on eastward propagating moisture mode (Λ = 0, -0.5, 1.5, and 3); other parameter are fixed (α = 0.25, Γ_q = -0.05).

Further, we explored the role of MCF in the development of planetary-scale instability and propagation of eastward moisture mode. For identifying the physical mechanism of MCF alone, we considered two possible cases, first the moist-neutral case (Γ_q = 0) and second case when moisture convergence feedback is off (Γ_q = 1), while keeping the constant values of EWF (Λ = 0.05) and MRT (α = 0.33). Figure 4a depicts the modified eastward moisture mode due to different Γ_q values. From this illustration, it is clear that the instability remains the same at planetary-scale wavelengths when the system is in either a moist-neutral case or without MCF. However, the frequency is modified in such a way that for a moist-neutral case, it is in the intraseasonal frequency range (blue circles). Without a moist convergence feedback case, the eastward moisture mode's frequency (blue dots) is reduced, and it is not in the range of observational time period. Corresponding growth rate curves are shown in Figure 4b. These curves demonstrate that for the moist-neutral case (blue dots), the growth rate of the eastward moisture mode slowly decreases with the wavenumber and gets damped at shorter wavelengths. Furthermore, the growth rate for the case without MCF is higher than the prior case but shows similar qualitative nature. The phase speed curves are shown in Figure 4c, and these results show that maximum phase speed is observed at the planetary-scale wavelength when the moist-neutral case is invoked. However, for the other case, it shows a very slow phase speed at similar wavelengths. Further, we analyzed the sensitivity of MCF by varying its value to Γ_q = -0.5 and -1. In comparison with the EWF, the MCF has negligible effects on the development of planetary-scale instability (Figure 4a). However, it is shown that there is a significant effect on dispersion relation at smaller wavelengths. It is clear that at the shorter wavelengths, the obtained mode becomes more damped, depending on the MCF value. Hence, MCF mainly acts to regulate the frequency of the

Preprints (www.preprints.org) | NOT PEER-REVIEWED | Posted: 8 August 2023 doi:10.20944/preprints202308.0626.v1

eastward moisture mode. We can observe the growth rate pattern of modified eastward moisture mode (Γ_q values -0.5 and -1) from Figure Figure 4b. The growth rate shows a peculiar behavior; it falls sharply with the wavenumber up to the planetary scale range and then increases for intermediate wavenumbers. Further, it becomes neutral for higher wavenumbers. Therefore, from this observation, it is clear that the MCF does not favor the planetary scale instability because the MCF-induced growth rate does not favor the longer wavelength but is rather significant at shorter wavelengths. Similarly, variations in the phase speed at longer wavelengths are not observed, but at shorter wavelengths, it decreases rapidly and becomes unrealistic. The results demonstrate that either of the feedback processes alone cannot establish the MJO-like signature. Although EWF introduces the eastward perturbation, it cannot reduce the frequency of eastward moisture mode at higher zonal wavenumbers, but the MCF regulates the frequency of the eastward moisture modes at large zonal wavenumbers.

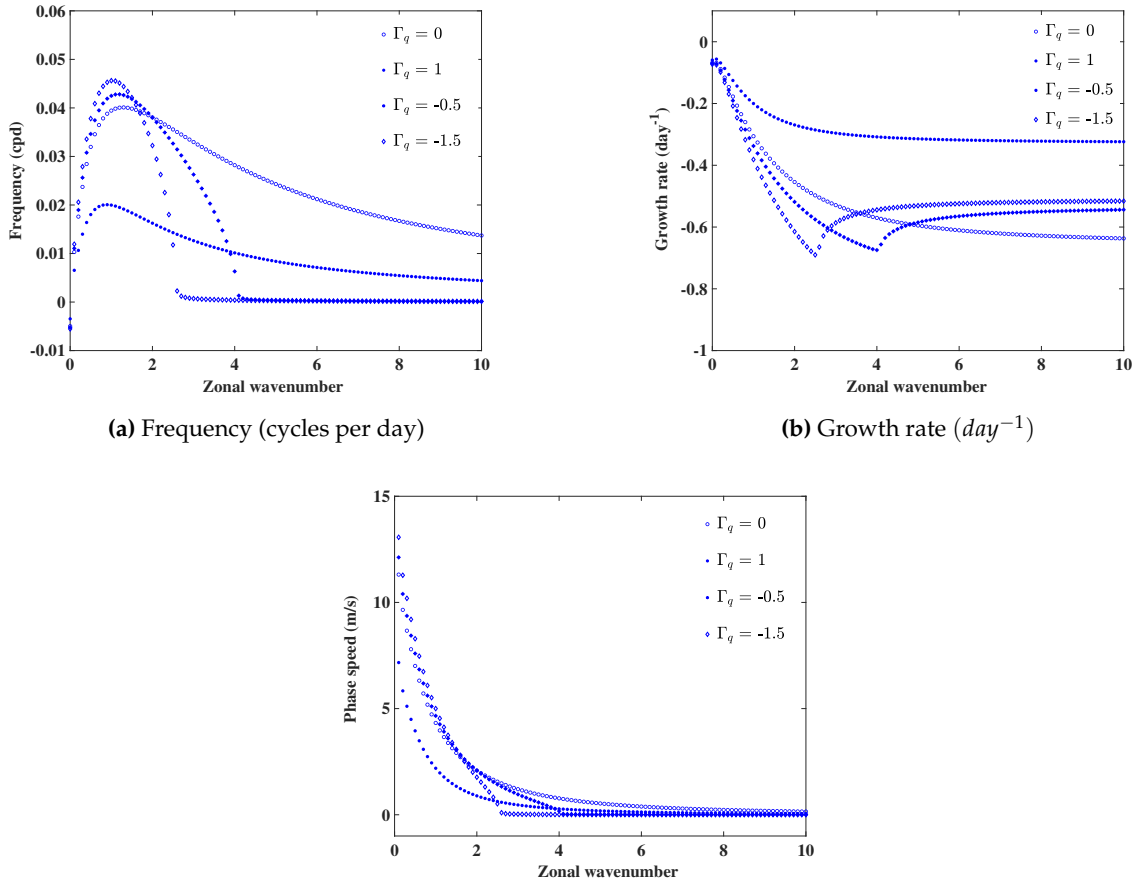

(a) Frequency (cycles per day)

(b) Growth rate (day^{-1})

(c) Phase speed (m/sec)

Figure 4. Role of MCF on eastward propagating moisture mode (Γ_q = 0, 1, -0.5, and -1); other parameter are fixed (α = 0.25, Λ = 0.05).

Finally, we explored the role of another significant model parameter, i.e., moisture relaxation time scale τ (α^-), which determines the dynamics of convective interactions through precipitational heating in the tropical atmosphere. We initially chose this to be one day based on physical arguments, and recent numerical model simulations by [46]. At this timescale, along with the active EWF and MCF, we simulated an unstable eastward moisture mode Figure 5. Further, we were interested in identifying the behavior of eastward moisture mode at different MRTs Figure 5a. For a short MRT (τ = 2 hours), the frequency of the solution increases with wavenumber and behaves like a moist-Kelvin wave. The growth rate decreases sharply with the wavenumber and further gets damped at smaller wavelengths Figure 5b. The phase speed reaches the maximum value (≈15 m/sec) at the planetary-scale wavenumber. Almost similar dispersion behavior is observed when MRT increases to

Preprints (www.preprints.org) | NOT PEER-REVIEWED | Posted: 8 August 2023 doi:10.20944/preprints202308.0626.v1

12 hours. The increase in MRT to 1.5 days results in a decrease in frequency in the intraseasonal range, with a peculiar dispersion relationship similar to the observed MJO-mode. In this case, the solution attains a maximum growth rate at longer wavelengths, decreases slowly with the wavenumber at the intermediate scale, and finally becomes stable for shorter wavelengths. Moreover, the phase speed is also in the range of 5-6 m/sec at planetary scale zonal wavenumbers. Further, increasing MRT values to 2.5 days decreases the frequency with an unrealistic phase speed and growth rate. These results agree with the existing models based on trio-interaction theory by [20]. However, with a convective adjustment scale of 12 hours, their simulated moisture mode results from a complex interaction among boundary layer convergence, CRF, and moisture processes.

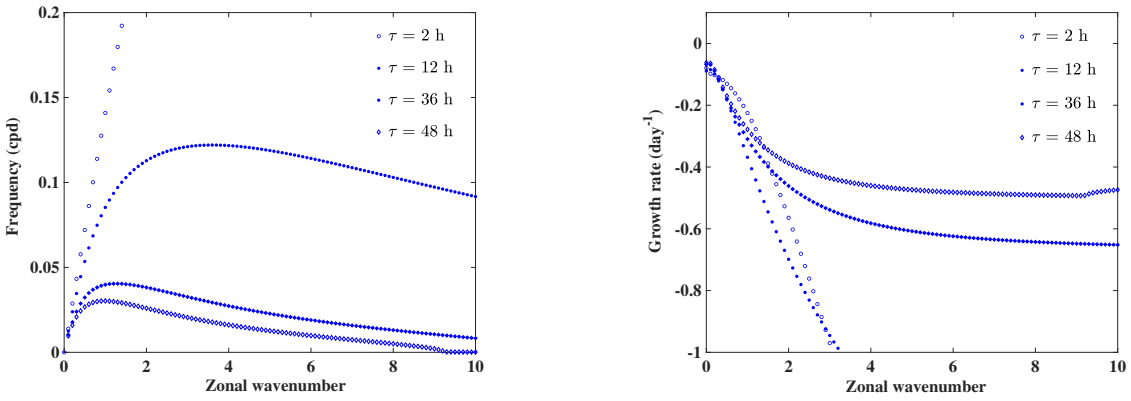

(a) Frequency (cycles per day)

(b) Growth rate (day^{-1})

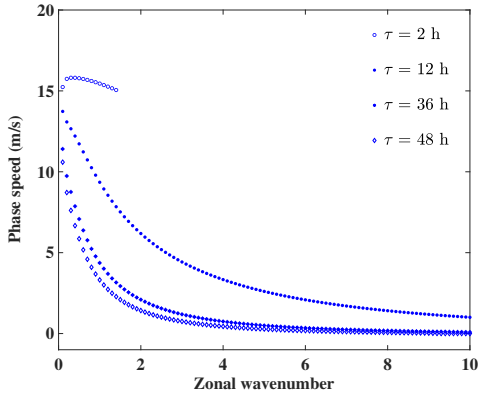

(c) Phase speed (m/sec)

Figure 5. Role of MRT on eastward propagating moisture mode (α = 0.23, 0.34, 0.68, and 1.37); other parameter are fixed (Λ = 0.05, Γ_q = -0.05).

4. Conclusions

In the present work, we investigated the influence of the EWF and MCF on the dispersive signature of low-frequency tropical intra-seasonal oscillation using a moisture-coupled, linear shallow-water model on the equatorial beta plane. We considered the linear evolution of precipitational heating and the unidirectional surface winds (easterly dominant) for analytical simplicity. With these minimum mechanisms, we search for the solutions intrinsic to the low-frequency regime of the tropical waveguide. The analytical dispersion relation gives two different unstable moisture modes (Figure 1). The first one is the westward moisture mode, and it closely resembles the traditional n=1 planetary-scale equatorial Rossby wave. The other solution is an eastward perturbation having the largest instability at longer wavelengths. This new moisture mode exhibits a characteristic dispersion behavior on an intra-seasonal time scale. i.e., its frequency is almost constant as a function of wavenumber, a

slow eastward propagation with a phase speed of around 5-6 m/sec, and shows a critical instability at planetary-scale wavelengths. All these characteristic features agree with the minimum criteria prescribed by Zhang *et al.* [14] for identifying theoretically simulated eastward mode as the MJO mode, and also consistent with the observational studies of Kiladis *et al.* [4]. Hence, we referred to this eastward moisture mode as a low-frequency intra-seasonal oscillation or MJO.

Further, we systematically scrutinized the influence of the moist-convective feedback processes on this eastward moisture mode, and we verified the necessity of each process in sustaining the planetary-scale instability, regulation in intra-seasonal frequency, and continuous eastward propagation. In this context, we conclude that the fundamental source for the existence of eastward moisture mode and its planetary-scale instability is evaporation wind feedback. Our model's eastward moisture mode is similar to the linear solutions obtained from established theoretical frameworks, such as WISHE and trio-interaction theory, despite the fact that we did not involve other complex interactions, such as cloud radiation feedback and boundary-layer dynamics. In conclusion, our model results confirmed that the moisture convergence feedback alone could not produce instability at longer wavelengths; however, it regulates the frequency and growth rates at shorter wavelengths. Similar to WISHE theory and the trio-interaction model, our model's simulation is also sensible to the moisture relaxation time scale, which decides whether the obtained mode is moist Kelvin mode or a new eastward moisture mode, considered to be MJO. The present model does not include the nonlinear evolution of the precipitation and related latent heat release, yet it can still deduce the fundamental characteristics of intra-seasonal oscillation. However, inclusion of nonlinear effects associated with precipitational heating, boundary layer dynamics, and other scale interactions are necessary for understanding the complex, multi-scale structure of the MJO.

Data Availability Statement: The paper is theoretical, and no data are used. Moreover, the plots were generated from the equations, as the model is purely analytical.

Funding: This research received no external funding.

Conflicts of Interest: The authors declare no conflict of interest.

References

1. Lau, W.K.M.; Waliser, D.E. *Intraseasonal variability in the atmosphere-ocean climate system*; Springer Science & Business Media, 2011.
2. Madden, R.A.; Julian, P.R. Detection of a 40–50 Day Oscillation in the Zonal Wind in the Tropical Pacific. *Journal of the Atmospheric Sciences* **1971**, *28*, 702–708. https://doi.org/10.1175/1520-0469(1971)028<0702:doadoi>2.0.co;2.
3. Madden, R.A.; Julian, P.R. Description of Global-Scale Circulation Cells in the Tropics with a 40–50 Day Period. *Journal of the Atmospheric Sciences* **1972**, *29*, 1109–1123. https://doi.org/10.1175/1520-0469(1972)029<1109:dogscc>2.0.co;2.
4. Kiladis, G.N.; Wheeler, M.C.; Haertel, P.T.; Straub, K.H.; Roundy, P.E. Convectively coupled equatorial waves. *Reviews of Geophysics* **2009**, *47*. https://doi.org/10.1029/2008rg000266.
5. Matsuno, T. Quasi-Geostrophic Motions in the Equatorial Area. *Journal of the Meteorological Society of Japan. Ser. II* **1966**, *44*, 25–43. https://doi.org/10.2151/jmsj1965.44.1_25.
6. Hendon, H.H.; Salby, M.L. The Life Cycle of the Madden–Julian Oscillation. *Journal of the Atmospheric Sciences* **1994**, *51*, 2225–2237. https://doi.org/10.1175/1520-0469(1994)051<2225:tlcotm>2.0.co;2.
7. Kiladis, G.N.; Straub, K.H.; Haertel, P.T. Zonal and Vertical Structure of the Madden–Julian Oscillation. *Journal of the Atmospheric Sciences* **2005**, *62*, 2790–2809. https://doi.org/10.1175/jas3520.1.
8. Ahn, M.S.; Kim, D.; Kang, D.; Lee, J.; Sperber, K.R.; Gleckler, P.J.; Jiang, X.; Ham, Y.G.; Kim, H. MJO Propagation Across the Maritime Continent: Are CMIP6 Models Better Than CMIP5 Models? *Geophysical Research Letters* **2020**, *47*. https://doi.org/10.1029/2020gl087250.
9. Kang, W.; Tziperman, E. The MJO-SSW Teleconnection: Interaction Between MJO-Forced Waves and the Midlatitude Jet. *Geophysical Research Letters* **2018**, *45*, 4400–4409. https://doi.org/10.1029/2018gl077937.
10. Zhang, C. Madden–Julian Oscillation: Bridging Weather and Climate. *Bulletin of the American Meteorological Society* **2013**, *94*, 1849–1870. https://doi.org/10.1175/bams-d-12-00026.1.

11. Liebmann, B.; Hartmann, D.L. An Observational Study of Tropical–Midlatitude Interaction on Intraseasonal Time Scales during Winter. *Journal of the Atmospheric Sciences* **1984**, *41*, 3333–3350. https://doi.org/10.1175/1520-0469(1984)041<3333:aosoti>2.0.co;2.
12. Biello, J.A.; Majda, A.J. A New Multiscale Model for the Madden–Julian Oscillation. *Journal of the Atmospheric Sciences* **2005**, *62*, 1694–1721. https://doi.org/10.1175/jas3455.1.
13. Majda, A.J.; Stechmann, S.N. A Simple Dynamical Model with Features of Convective Momentum Transport. *Journal of the Atmospheric Sciences* **2009**, *66*, 373–392. https://doi.org/10.1175/2008jas2805.1.
14. Zhang, C.; Adames, Á.F.; Khouider, B.; Wang, B.; Yang, D. Four Theories of the Madden-Julian Oscillation. *Reviews of Geophysics* **2020**, *58*. https://doi.org/10.1029/2019rg000685.
15. Raymond, D.J.; Fuchs, Ž. Moisture Modes and the Madden–Julian Oscillation. *Journal of Climate* **2009**, *22*, 3031–3046. https://doi.org/10.1175/2008jcli2739.1.
16. Hannah, W.M.; Maloney, E.D. The Role of Moisture–Convection Feedbacks in Simulating the Madden–Julian Oscillation. *Journal of Climate* **2011**, *24*, 2754–2770. https://doi.org/10.1175/2011jcli3803.1.
17. Sobel, A.; Maloney, E. An Idealized Semi-Empirical Framework for Modeling the Madden–Julian Oscillation. *Journal of the Atmospheric Sciences* **2012**, *69*, 1691–1705. https://doi.org/10.1175/jas-d-11-0118.1.
18. Adames, Á.F.; Kim, D. The MJO as a Dispersive, Convectively Coupled Moisture Wave: Theory and Observations. *Journal of the Atmospheric Sciences* **2016**, *73*, 913–941. https://doi.org/10.1175/jas-d-15-0170.1.
19. Jiang, X.; Adames, Á.F.; Zhao, M.; Waliser, D.; Maloney, E. A Unified Moisture Mode Framework for Seasonality of the Madden–Julian Oscillation. *Journal of Climate* **2018**, *31*, 4215–4224. https://doi.org/10.1175/jcli-d-17-0671.1.
20. Wang, B.; Liu, F.; Chen, G. A trio-interaction theory for Madden–Julian oscillation. *Geoscience Letters* **2016**, *3*. https://doi.org/10.1186/s40562-016-0066-z.
21. Emanuel, K.A. An Air-Sea Interaction Model of Intraseasonal Oscillations in the Tropics. *Journal of the Atmospheric Sciences* **1987**, *44*, 2324–2340. https://doi.org/10.1175/1520-0469(1987)044<2324:aasimo>2.0.co;2.
22. Fuchs, Z.; Raymond, D.J. Large-Scale Modes in a Rotating Atmosphere with Radiative–Convective Instability and WISHE. *Journal of the Atmospheric Sciences* **2005**, *62*, 4084–4094. https://doi.org/10.1175/jas3582.1.
23. Fuchs, Ž.; Raymond, D.J. A simple model of intraseasonal oscillations. *Journal of Advances in Modeling Earth Systems* **2017**, *9*, 1195–1211. https://doi.org/10.1002/2017ms000963.
24. Khairoutdinov, M.F.; Emanuel, K. Intraseasonal Variability in a Cloud-Permitting Near-Global Equatorial Aquaplanet Model. *Journal of the Atmospheric Sciences* **2018**, *75*, 4337–4355. https://doi.org/10.1175/jas-d-18-0152.1.
25. Yang, D.; Ingersoll, A.P. Triggered Convection, Gravity Waves, and the MJO: A Shallow-Water Model. *Journal of the Atmospheric Sciences* **2013**, *70*, 2476–2486. https://doi.org/10.1175/jas-d-12-0255.1.
26. Yano, J.I.; Tribbia, J.J. Tropical Atmospheric Madden–Julian Oscillation: A Strongly Nonlinear Free Solitary Rossby Wave? *Journal of the Atmospheric Sciences* **2017**, *74*, 3473–3489. https://doi.org/10.1175/jas-d-16-0319.1.
27. Rostami, M.; Zeitlin, V. Eastward-moving convection-enhanced modons in shallow water in the equatorial tangent plane. *Physics of Fluids* **2019**, *31*, 021701. https://doi.org/10.1063/1.5080415.
28. Charney, J.G.; Eliassen, A. On the Growth of the Hurricane Depression. *Journal of the Atmospheric Sciences* **1964**, *21*, 68–75. https://doi.org/10.1175/1520-0469(1964)021<0068:otgoth>2.0.co;2.
29. Ooyama, K.V. Conceptual Evolution of the Theory and Modeling of the Tropical Cyclone. *Journal of the Meteorological Society of Japan. Ser. II* **1982**, *60*, 369–380. https://doi.org/10.2151/jmsj1965.60.1_369.
30. Emanuel, K.A.; Neelin, J.D.; Bretherton, C.S. On large-scale circulations in convecting atmospheres. *Quarterly Journal of the Royal Meteorological Society* **1994**, *120*, 1111–1143. https://doi.org/10.1002/qj.49712051902.
31. Lindzen, R.S. Wave-CISK in the Tropics. *Journal of the Atmospheric Sciences* **1974**, *31*, 156–179. https://doi.org/10.1175/1520-0469(1974)031<0156:wcitt>2.0.co;2.
32. Moskowitz, B.M.; Bretherton, C.S. An Analysis of Frictional Feedback on a Moist Equatorial Kelvin Mode. *Journal of the Atmospheric Sciences* **2000**, *57*, 2188–2206. https://doi.org/10.1175/1520-0469(2000)057<2188:aaoffo>2.0.co;2.
33. Betts, A.K. Saturation Point Analysis of Moist Convective Overturning. *Journal of the Atmospheric Sciences* **1982**, *39*, 1484–1505. https://doi.org/10.1175/1520-0469(1982)039<1484:spaomc>2.0.co;2.

34. Xu, K.M.; Emanuel, K.A. Is the Tropical Atmosphere Conditionally Unstable? *Monthly Weather Review* **1989**, *117*, 1471–1479. https://doi.org/10.1175/1520-0493(1989)117<1471:ittacu>2.0.co;2.
35. Fuchs-Stone, Ž.; Emanuel, K. Sensitivity of Linear Models of the Madden–Julian Oscillation to Convective Representation. *Journal of the Atmospheric Sciences* **2022**, *79*, 1575–1584. https://doi.org/10.1175/jas-d-21-0165.1.
36. Hu, Q.; Randall, D.A. Low-Frequency Oscillations in Radiative-Convective Systems. *Journal of the Atmospheric Sciences* **1994**, *51*, 1089–1099. https://doi.org/10.1175/1520-0469(1994)051<1089:lfoirc>2.0.co;2.
37. Cao, C.; Liu, F.; Wu, Z. Role of cloud radiative feedback in the Madden–Julian oscillation dynamics: a trio-interaction model analysis. *Theoretical and Applied Climatology* **2021**, *145*, 489–499. https://doi.org/10.1007/s00704-021-03641-w.
38. Nakazawa, T. Tropical Super Clusters within Intraseasonal Variations over the Western Pacific. *Journal of the Meteorological Society of Japan. Ser. II* **1988**, *66*, 823–839. https://doi.org/10.2151/jmsj1965.66.6_823.
39. Goswami, P.; Goswami, B.N. Modification of n= 0 Equatorial Waves Due to Interaction between Convection and Dynamics. *Journal of the Atmospheric Sciences* **1991**, *48*, 2231–2244. https://doi.org/10.1175/1520-0469(1991)048<2231:moewdt>2.0.co;2.
40. Goswami, P.; Mathew, V. A Mechanism of Scale Selection in Tropical Circulation at Observed Intraseasonal Frequencies. *Journal of the Atmospheric Sciences* **1994**, *51*, 3155–3166. https://doi.org/10.1175/1520-0469(1994)051<3155:amossi>2.0.co;2.
41. Bretherton, C.S.; Peters, M.E.; Back, L.E. Relationships between Water Vapor Path and Precipitation over the Tropical Oceans. *Journal of Climate* **2004**, *17*, 1517–1528. https://doi.org/10.1175/1520-0442(2004)017<1517:rbwvpa>2.0.co;2.
42. Neelin, J.D.; Held, I.M.; Cook, K.H. Evaporation-Wind Feedback and Low-Frequency Variability in the Tropical Atmosphere. *Journal of the Atmospheric Sciences* **1987**, *44*, 2341–2348. https://doi.org/10.1175/1520-0469(1987)044<2341:ewfalf>2.0.co;2.
43. Vallis, G.K. The Trouble with Water: Condensation, Circulation and Climate. *The European Physical Journal Plus* **2020**, *135*. https://doi.org/10.1140/epjp/s13360-020-00493-7.
44. Emanuel, K. Slow Modes of the Equatorial Waveguide. *Journal of the Atmospheric Sciences* **2020**, *77*, 1575–1582. https://doi.org/10.1175/jas-d-19-0281.1.
45. Fuchs-Stone, Ž. WISHE-Moisture Mode in a Vertically Resolved Model. *Journal of Advances in Modeling Earth Systems* **2020**, *12*. https://doi.org/10.1029/2019ms001839.
46. Bretherton, C.S.; Sobel, A.H. The Gill Model and the Weak Temperature Gradient Approximation. *Journal of the Atmospheric Sciences* **2003**, *60*, 451–460. https://doi.org/10.1175/1520-0469(2003)060<0451:tgmatw>2.0.co;2.